

Electronic structure and symmetry of valence states of epitaxial NiTiSn and NiZr_{0.5}Hf_{0.5}Sn thin films by hard x-ray photoelectron spectroscopy.

Xeniya Kozina,¹ Tino Jaeger,² Siham Ouardi,¹ Andrei Gloskowskij,¹ Gregory Stryganyuk,¹ Gerhard Jakob,² Takeharu Sugiyama,³ Eiji Ikenaga,³ Gerhard H. Fecher,^{1,4, a)} and Claudia Felser^{1,4}

¹⁾*Institut für Anorganische und Analytische Chemie, Johannes Gutenberg - Universität, 55099 Mainz, Germany.*

²⁾*Institut für Physik, Johannes Gutenberg - Universität, 55099 Mainz, Germany.*

³⁾*Japan Synchrotron Radiation Research Institute (JASRI), SPring-8, Hyogo 679-5198, Japan*

⁴⁾*Max Planck Institute for Chemical Physics of Solids, 01187 Dresden, Germany.*

(Dated: 31 August 2018)

The electronic band structure of thin films and superlattices made of Heusler compounds with NiTiSn and NiZr_{0.5}Hf_{0.5}Sn composition was studied by means of polarization dependent hard x-ray photoelectron spectroscopy. The linear dichroism allowed to distinguish the symmetry of the valence states of the different types of layered structures. The films exhibit a larger amount of "in-gap" states compared to bulk samples. It is shown that the films and superlattices grown with NiTiSn as starting layer exhibit an electronic structure close to bulk materials.

Keywords: Thermoelectric materials, Superlattice, Electronic structure, Dichroism in photoemission, Photoelectron spectroscopy

^{a)}Electronic mail: fecher@uni-mainz.de

The progressively growing interest in exploration and design of the materials exhibiting thermoelectric properties is mediated by their potential applications in new environment friendly industrial technologies for power generation and refrigeration¹. As the efficiency of a thermoelectric device solely depends on the dimensionless figure of merit $ZT = S^2\sigma\kappa^{-1}$ at operating temperature, the most interesting materials are those with high ZT , which is, in turn, defined by thermopower S , electric conductivity σ and thermal conductivity κ . Due to the unique tunability of properties, thermal and chemical stability, non-toxicity and ease in synthesis, among other half-Heusler compounds the NiXSn based family of compounds and their solid solutions have become the most perspective ones for reaching high ZT values²⁻⁵. Many attempts were made towards optimization of ZT via enlarging either S or σ ^{4,6}. Alternatively a reduction of κ allows significantly to rise ZT values, as it was demonstrated for $YX_{0.5}X'_{0.5}Z$ family of half-Heusler compounds^{3,7,8}.

Boundary scattering of electrons and phonons play a major role in further suppression of the thermal conductivity in polycrystalline materials⁹ and thin film superlattices. In the latter case the phonons are scattered at the superlattice interfaces when their mean free path is shorter than the period of the superlattice leading to low values of the cross-plane κ ¹⁰. Improvement of the quality of such multilayer stacks as it was previously demonstrated for epitaxial NiTiSn/NiZr_{0.5}Hf_{0.5}Sn superlattices¹¹ will create new options for producing high performance thermoelectric devices.

To improve the transport properties of the materials it is necessary to understand and explore their electronic structure close to the Fermi energy (ϵ_F). Hard x-ray photoelectron spectroscopy (HAXPES) is a powerful method to probe both chemical states and electronic structure of bulk materials and buried layers in a non-destructive way^{12,13}. The combination of HAXPES with polarized radiation for excitation significantly extends its applicability. The use of linearly s and p polarized light in HAXPES enables the analysis of the symmetry of bulk electronic states¹⁴. In the present study the valence band electronic structure of NiTiSn/NiZr_{0.5}Hf_{0.5}Sn superlattices were investigated by means of HAXPES and linear dichroism.

For the present study, multilayer stacks consisting of alternating NiTiSn and NiZr_{0.5}Hf_{0.5}Sn layers were deposited by means of dc-sputtering. The details of fabrication and characterization of the samples are described in Reference¹¹. Sketches of the investigated thin film, bilayer, and superlattice samples are shown in Fig. 1. The topmost AlO_x layer serves as a

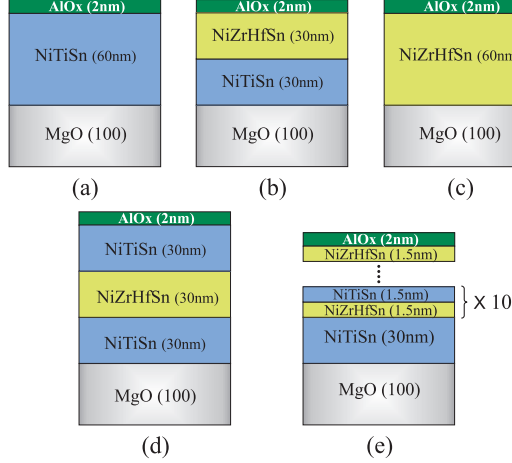


FIG. 1. Sketch of the sample structures. The layers in (a), (b) and (c) correspond to the 30-nm-thick films of NiTiSn and NiZr_{0.5}Hf_{0.5}Sn compounds grown on different buffer layers. (d) presents a bilayer sample and (e) shows the superlattice.

protective cap preventing the oxidation and degradation of the thin films.

The HAXPES experiment was performed at BL47XU of Spring-8 (Japan) using 7.940 keV linearly polarized photons for excitation. Vertical (s) direction of polarization was achieved by means of a in-vacuum phase retarder based on a 600- μ m-thick diamond crystal with a degree of polarization above 90 %. Horizontal (p) polarization was obtained directly from the undulator without any additional polarization optics. The energy resolution was set to 250 meV and was verified by spectra of the Au valence band at the ϵ_F . Gracing incidence – normal emission geometry was used ($\theta=2^\circ$) that ensures that the polarization vector was nearly parallel (p) or perpendicular (s) to the surface normal. For further details on HAXPES experiment see^{14,15}.

Fig. 2(a) presents the valence band spectra of NiTiSn and NiZr_{0.5}Hf_{0.5}Sn 30-nm-thick films grown on different buffer layers (NiTiSn or NiZr_{0.5}Hf_{0.5}Sn (see Fig. 1 (a), (b) and (c))). The spectra of the materials grown on a NiTiSn buffer reveal clearly narrow structures originating from the band structure of the Heusler compounds. The structure at lower binding energies corresponds to the d - states. They are separated by the intrinsic Heusler sp -hybridization gap (at about -6 eV) from the s -states. In the range above -6 eV the 4-peak- structure peculiar to NiXSn compounds is clearly resolved. Such shape of the energy distribution curve is formed mainly by the partial density of Ni-3d states as was shown previously (see References^{14,16,17} for the calculated density of states (DOS)). The contribution of the Sn s

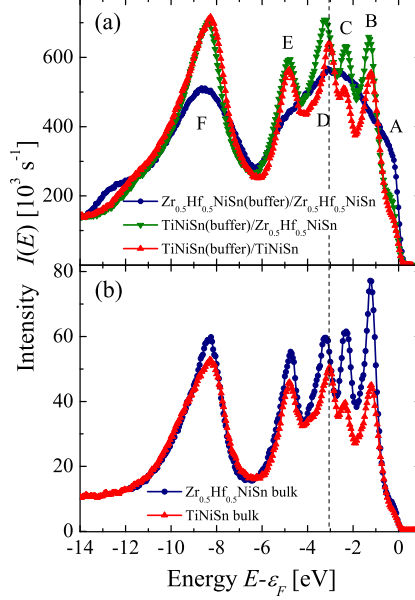


FIG. 2. Valence band spectra of the single NiTiSn and $\text{NiZr}_{0.5}\text{Hf}_{0.5}\text{Sn}$ films grown on different buffer layers (a) compared to polycrystalline NiTiSn and $\text{NiZr}_{0.5}\text{Hf}_{0.5}\text{Sn}$ bulk samples (b). (Note that the additional intensity at below -10 eV seen in a) emerges from the AlO_x cap layer.)

states gives rise to the broad peak at -8.26 eV (peak F). Apparently the intensity of s -states becomes comparable with that of d -states at about 8 keV excitation energy. Such a behavior is a direct consequence of different cross sections for s and d states.

The peaks positions of NiTiSn and $\text{NiZr}_{0.5}\text{Hf}_{0.5}\text{Sn}$ films grown on a NiTiSn buffer agree well with those of polycrystalline NiTiSn and $\text{NiZr}_{0.5}\text{Hf}_{0.5}\text{Sn}$ bulk samples shown in Fig. 2(b). As it was demonstrated before^{14,18}, the intensity of peaks B (-1.21 eV) and C (-2.41 eV) undergoes drastic changes. When going from NiTiSn to $\text{NiZr}_{0.5}\text{Hf}_{0.5}\text{Sn}$, i. e. by substitution of Ti atoms by (Zr,Hf), peaks B and C are increased. This follows from the fact that the Ti $3d$ partial DOS contributes significantly to the total DOS in this energy range along with the Ni $3d$ states. Larger cross sections for Zr $4d$ and Hf $5d$ states compared to the Ti $3d$ states enhance the peaks. Moreover, feature D shifts towards higher binding energies by 0.21 eV in the spectra of both bulk samples and thin films when Ti is substituted by (Zr,Hf). This correlation in the spectra of the epitaxially grown thin films and the pure polycrystalline samples together with the agreement with previously reported results implies the formation of a well ordered crystalline C_{1b} structure in the films of both compounds when grown on a NiTiSn buffer layer.

For both compounds one observes the appearance of "*in-gap*" states close to ϵ_F (feature A). Substitution of Ti atoms with (Zr,Hf) leads to an increase of "*in-gap*" states in both thin films and bulk samples that is in a good agreement with recent work¹⁸. Such states are attributed to the disorder at the Ti-site, viz. formation of the antisites of Ti atoms with the vacancies¹⁹. They are responsible for the remarkable thermoelectric properties of the materials. The relatively high amount of "*in-gap*" states in the thin films compared with the bulk materials can be explained by the presence of additional crystalline defects in the thin films induced by lattice strain, interface states with broken symmetry, or interdiffusion of atoms in conjugated layers. NiZr_{0.5}Hf_{0.5}Sn grown on a NiZr_{0.5}Hf_{0.5}Sn buffer (Fig. 2(a)) has obviously a high degree of disorder as is revealed from both smeared out valence band and completely closed band gap.

Further investigations were performed on bilayers and superlattices (Fig. 1 (d), (e)). Both, *p*- and *s*-polarized, hard x-rays were used for excitation. The photoelectron spectra of both samples (Fig. 3) are typical for the electronic structure of the compounds, as described above. The high probing depth in the order of tens of nanometers allows to obtain the information from several 1.5-nm-thick layers of the superlattice. Their contribution to the total signal is nonequivalent as is seen in Fig. 3. One notices a relative redistribution of peaks B, C, and D when comparing the spectra taken with both orthogonal polarization. A clear enhancement of the signals from the B and C states – similar to the NiZr_{0.5}Hf_{0.5}Sn sample – is explained by the presence of the topmost 1.5 nm-thick NiZr_{0.5}Hf_{0.5}Sn layer in the superlattice. Here, most of the obtained signal is attributed to the NiZr_{0.5}Hf_{0.5}Sn layer whereas the intensity from the underlying and other layers is damped due to increased inelastic scattering probability for electrons passing larger distances through the upper layers of the structure.

The spectra shown in Fig. 3 were normalized to the secondary electron background at about -14 eV to account for different intensities for different kind of polarization (see also¹⁴). Substantial changes of the spectra from both samples are quite obvious when the polarization is switched from *p* to *s*. In both cases the peak at -8.31 eV arising from Sn *s* (*a*₁) states is enhanced with *p*-polarized photons, while the intensity of the *d*-part of the spectra is lowered. Namely the features originating from *e* and *t*₂ states (-2.36 eV) and *t*₂ states (-3.06 eV) of Ni as well as *e* and *t*₂ states (-1.3 eV) of Ti are enhanced when using *p*-polarized photons for excitation¹⁹. The relative change in the intensity of peak E arising from *t*₁ states of Ni and Ti is larger in the superlattice sample (see difference curve in Fig. 3(b)). This is due to

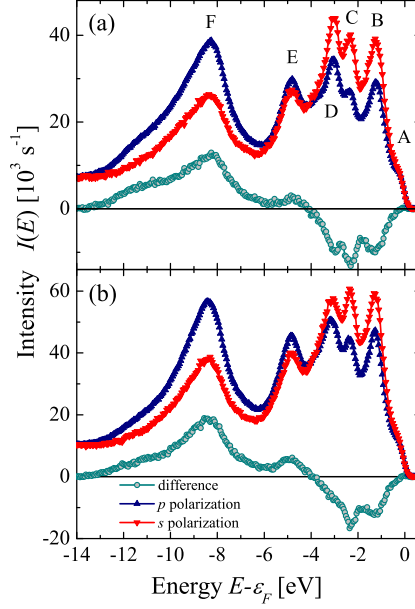


FIG. 3. Polarization-dependent valence band spectra of a NiZr_{0.5}Hf_{0.5}Sn/NiTiSn bilayer (a) and the NiTiSn/NiZr_{0.5}Hf_{0.5}Sn superlattice (b). The spectra obtained with *s* and *p* polarized x-rays are shown together with the difference curves.

the different overlying material in the two samples and therefore a increased contribution of states from Zr and Hf. In the bilayer sample the enhancement of the relative change in peak D at -3.06 eV giving a sharper feature in the difference curve (Fig. 3(a)) is caused mainly by changes of the cross sections for t_2 states of Ni similarly as it was observed previously for polycrystalline NiTiSn¹⁴. This is in a good agreement with the present case as the 30 nm overlying layer mostly contributes to the overall signal obtained from the bilayer structure. From the polarization dependence it is also concluded that the *in-gap* states have *d*-type character.

summary, the investigation of electronic properties of thin films as well as superlattices of NiTiSn and NiZr_{0.5}Hf_{0.5}Sn thermoelectric materials were performed by means of HAXPES. The polarization dependent HAXPES investigation allowed clearly to distinguish the states of different symmetry contributing to the total DOS in the valence band region in the pure NiTiSn and NiZr_{0.5}Hf_{0.5}Sn thin films. The impact of the different materials could even be resolved in the complex multilayered structures. Utilizing of NiTiSn as buffer layer for epitaxial growth of the different thin films and superlattices of both materials results in a high quality of the crystalline structure. The studies showed the appearance of "*in-gap*"

d-states in both compounds that may be mediated by disorder at the interfaces and possible strain effects common for thin film structures. The "*in-gap*" states can serve as a tool for artificial tuning of the thermoelectric properties in thin films – in particular an increase of the conductivity –, as was shown already for bulk materials.

Financial support by the DFG (Fe633/8-1 and Ja821/4-1 in SPP 1386) is gratefully acknowledged. HAXPES was performed at BL47XU of SPring-8 with approval of JASRI (Proposals No. 2011A1464, 2010A0017).

REFERENCES

- ¹J. R. Sootsman, D. Y. Chung, and M. G. Kanatzidis, *Angew. Chem. int. Ed.* **48**, 8616 (2009).
- ²F. G. Aliev, V. V. Kozyrkov, V. V. Moschalkov, R. V. Skolozdra, and K. Durczewski, *Z. Physik* **B80**, 353 (1990).
- ³S. Sakurada and N. Shutoh, *Appl. Phys. Lett.* **86**, 082105 (2005).
- ⁴N. Shutoh and S. Sakurada, *J. Alloys Comp.* **389**, 204 (2005).
- ⁵L. Chaput, J. Tobola, P. Pécheur, and H. Scherrer, *Phys. Rev. B* **73**, 045121 (2006).
- ⁶M. Schwall and B. Balke, *Appl. Phys. Lett.* **98**, 042106 (2011).
- ⁷H. Hohl, A. P. Ramirez, C. Goldman, G. Ernst, B. Wölfing, and E. Bucher, *J. Phys.: Condens. Matter* **11**, 1697 (1999).
- ⁸Q. Shen, L. Chen, T. Goto, T. Hirai, J. Yang, G. P. Meisner, and C. Uher, *Appl. Phys. Lett.* **79**, 25 (2001).
- ⁹N. Savvides and H. J. Goldsmid, *J. Phys. C: Solid St. Phys.* **13**, 4657 (1980).
- ¹⁰B. Yanga, W. L. Liu, J. L. Liu, K. L. Wang, and G. Chen, *Appl. Phys. Lett.* **81**, 3588 (2002).
- ¹¹T. Jaeger, C. Mix, M. Schwall, X. Kozina, J. Barth, B. Balke, M. Finsterbusch, Y. U. Idzerda, C. Felser, and G. Jakob, *Thin Solid Films* **XX**, XX (2011).
- ¹²G. H. Fecher, B. Balke, A. Gloskowskii, S. Ouardi, C. Felser, T. Ishikawa, M. Yamamoto, Y. Yamashita, H. Yoshikawa, S. Ueda, and K. Kobayashi, *Appl. Phys. Lett.* **92**, 193513 (2008).
- ¹³X. Kozina, S. Ouardi, B. Balke, G. Stryganyuk, G. H. Fecher, C. Felser, S. Ikeda, H. Ohno, and E. Ikenaga, *Appl. Phys. Lett.* **96**, 072105 (2010).

- ¹⁴S. Ouardi, G. H. Fecher, X. Kozina, G. Stryganyuk, B. Balke, C. Felser, E. Ikenaga, T. Sugiyama, N. Kawamura, M. Suzuki, and K. Kobayashi, *Phys. Rev. Lett.* **107**, 036402 (2011).
- ¹⁵X. Kozina, G. H. Fecher, G. Stryganyuk, S. Ouardi, B. Balke, C. Felser, G. Schönhense, E. Ikenaga, T. Sugiyama, N. Kawamura, M. Suzuki, T. Taira, T. Uemura, M. Yamamoto, H. Sukegawa, W. Wang, K. Inomata, and K. Kobayashi, *Phys. Rev. B* **84**, 054449 (2011).
- ¹⁶J. Tobola, J. Pierre, S. Kaprzyk, R. V. Skolozdra, and M. A. Kouacou, *J. Phys.: Condens. Matter* **10**, 1013 (1998).
- ¹⁷J. Pierre, R. V. Skolozdra, J. Tobola, S. Kaprzyk, C. Hordequin, M. A. Kouacou, I. Karla, R. Currat, and E. Lelièvre-Berna, *J. Alloys Comp.* **262 - 263**, 101 (1997).
- ¹⁸K. Miyamoto, A. Kimura, K. Sakamoto, M. Ye, Y. Cui, K. Shimada, H. Namatame, M. Taniguchi, S. i. Fujimori, Y. Saitoh, E. Ikenaga, K. Kobayashi, J. Tadano, and T. Kanomata, *Appl. Phys. Exp.* **1**, 081901 (2008).
- ¹⁹S. Ouardi, G. H. Fecher, B. Balke, X. Kozina, G. Stryganyuk, C. Felser, S. Lowitzer, D. Ködderitzsch, H. Ebert, and E. Ikenaga, *Phys. Rev. B* **82**, 085108 (2010).